IOPscience iopscience.iop.org

Home Search Collections Journals About Contact us My IOPscience

Electronic properties of nanowire superlattices in the presence of strain and magnetic-field effects

This article has been downloaded from IOPscience. Please scroll down to see the full text article.

2008 J. Phys.: Condens. Matter 20 345216

(http://iopscience.iop.org/0953-8984/20/34/345216)

View the table of contents for this issue, or go to the journal homepage for more

Download details:
IP Address: 129.252.86.83
The article was downloaded on 29/05/2010 at 13:57

Please note that terms and conditions apply.

IOP PUBLISHING JOURNAL OF PHYSICS: CONDENSED MATTER

J. Phys.: Condens. Matter **20** (2008) 345216 (6pp) doi:10.1088/0953-8984/20/34/345216

Electronic properties of nanowire superlattices in the presence of strain and magnetic-field effects

M Willatzen[1] **and L C Lew Yan Voon**

Department of Physics, Wright State University, 3640 Colonel Glenn Highway, Dayton, OH 45435-0001, USA

E-mail: willatzen@mci.sdu.dk

Received 11 April 2008, in final form 27 June 2008
Published 1 August 2008
Online at stacks.iop.org/JPhysCM/20/345216

Abstract

A calculation of the effective electron barrier potential in quantum-wire superlattices subject to magnetic-field and strain effects is presented. It is shown that, besides the lateral-confinement contributions to the barrier potential emphasized by the authors in earlier work (Lew Yan Voon and Willatzen 2003 *J. Appl. Phys.* **93** 9997; Lew Yan Voon *et al* 2004 *J. Appl. Phys.* **96** 4660), strong contributions from strain (lattice mismatch) may be present as well. This is due to the fact that strain values can be several percent in heterostructures while electron deformation potentials are of the order of 10 eV. It is also shown that Landau and Landé magnetic-field contributions become important at magnetic fields of 10 T or higher. The driving force behind the lateral-confinement and the Landau magnetic-field contributions is the same, namely, the electron effective-mass difference in the two material constituents forming the superlattice structure; however, the dependences of the two contributions on lateral dimensions are inverse squared and squared, respectively. Similarly, the driving force behind the Landé magnetic-field contribution, being independent of lateral dimensions, is the difference in electron g factors between the two material constituents. We note that, for InAs/GaAs nanowire superlattices, it is possible to tune the effective barrier potential around 0 for cross-sectional dimensions of 5–6 nm by use of a magnetic field. Further, since the effective barrier potential is different for spin-up and spin-down polarized electrons, magnetic-field tuning can be used to separate spin-up and spin-down electrons in quantum-wire superlattices.

(Some figures in this article are in colour only in the electronic version)

1. Introduction

The spatial localization of the electronic states plays a fundamental role in defining the properties of nanostructures. For example, this determines the quantum-confinement energy or the strength of the optical transitions in optoelectronic devices. One of the earliest approaches to engineering the electronic wavefunction was by designing quantum-well structures [1]. Heterojunctions define which material is the well and which one is the barrier. For an AlAs/GaAs heterostructure, for example, GaAs (AlAs) is the well (barrier) material.

[1] Permanent address: Mads Clausen Institute, University of Southern Denmark, Alsion 2, DK-6400 Sønderborg, Denmark.

In 2002, modulated nanowires were first synthesized by four different groups [2–5]. One peculiar property predicted by us in 2003 is that the lateral size of the nanostructures can induce a transformational change in the electron localization equivalent to a well-barrier inversion [6, 7]. This effect has since been verified by another group [8]. The largest wire diameter we obtained for unstrained systems when there is an inversion for the conduction electrons is about 4 nm; unfortunately, modulated nanowires that small have not yet been made. This, therefore, raises the question as to how one can obtain larger critical radii. In addition, it would be useful if one could develop a solution that allows for tunability, with potential device applications. The above reasons have led us to explore the impact of strain and of a magnetic field on the

 © 2008 IOP Publishing Ltd Printed in the UK

electron localization properties of modulated semiconductor nanowires. It should be noted that both strain [9] and magnetic field [10] separately have been shown to lead to the possibility of a type-I to type-II transition in quantum wells. However, the magnetic case used a diluted magnetic semiconductor and none of these other works had provided a detailed theoretical analysis of the origin of the change in the electron localization. In the following, we will first present the general theory for the conduction electron in wide bandgap materials and then apply it to a few cases. The goal is to see how one can increase the critical size for inversion by the proper choice of material system and external magnetic field.

2. Quantum-wire superlattice problem in the presence of a magnetic field

Let us consider the case where the magnetic field is oriented along the z axis, i.e. $\theta = 0$. We shall further consider the quantum-wire superlattice direction to be the z axis. Hence, electrons are confined along the x and y axes assumed to be within the intervals $[0; L_x]$ and $[0; L_y]$, respectively. The envelope-function Hamiltonian is, allowing for a z-dependent effective mass:

$$H = \frac{p_x^2}{2m_e(z)} + \frac{1}{2m_e(z)}\left(p_y + eBx\right)^2 + \frac{1}{2}p_z\frac{1}{m_e(z)}p_z + V_{\rm conf}(z) + \tfrac{1}{2}g^*(z)\mu_B B, \tag{1}$$

where $\mathbf{p} = (p_x, p_y, p_z)$, $\mathbf{r} = (x, y, z)$, e, m_e, $V_{\rm conf}$, g^*, μ_B, B and $\boldsymbol{\sigma}$ are the electron momentum, the electron position, the absolute value of the electron charge, the electron effective mass, the conduction band edge potential, the electron effective Landé g factor, the Bohr magneton ($\frac{e\hbar}{2m_0}$), the magnetic field and the Pauli spin matrices, respectively. Multiplying equation (1) by $m_e(z)$ and writing for the envelope function ($H\psi = E\psi$)

$$\psi(x, y, z) = f(x, y)g(z), \tag{2}$$

we find

$$\frac{m_e(z)}{g(z)}\left[\frac{1}{2}p_z\frac{1}{m_e(z)}p_z + V_{\rm conf}(z) \pm \frac{1}{2}g^*(z)\mu_B B - E\right]g(z) = -\frac{1}{f(x,y)}\left[\frac{p_x^2}{2} + \frac{1}{2}\left(p_y + eBx\right)^2\right]f(x,y) \equiv \lambda^2, \tag{3}$$

where λ is a separation constant.

The second equality in equation (3) can be rewritten as

$$H_{xy}f(x,y) = \left(H_{xy,0} + H_{xy,1}\right)f(x,y) = \lambda^2 f(x,y), \tag{4}$$

$$H_{xy,0} = \frac{\hbar^2}{2}\left(\frac{\partial^2}{\partial x^2} + \frac{\partial^2}{\partial y^2}\right), \tag{5}$$

$$H_{xy,1} = \mathrm{i}\hbar eBx\frac{\partial}{\partial y} - \frac{1}{2}e^2B^2x^2. \tag{6}$$

We seek to investigate the effect of the magnetic field, i.e. $H_{xy,1}$ using perturbation theory. This is possible if dimensions L_x and L_y as well as the magnetic-field strength B are small since then the influence of $H_{xy,1}$ on eigenvalues is small compared to the separation of unperturbed eigenvalues of $H_{xy,0}$. Obviously, the first term in $H_{xy,1}$ does not contribute in first-order perturbation theory, since (normalized) eigenstates $f_{0,mn}$ of the unperturbed differential equation:

$$H_{xy,0}f_{0,mn}(x,y) = \lambda_{0,mn}^2 f_{0,mn}(x,y), \tag{7}$$

are

$$f_{0,mn}(x,y) = f_{0x,m}(x)f_{0y,n}(y), \tag{8}$$

$$f_{0x,m}(x) = \sqrt{\frac{2}{L_x}}\sin\left(\frac{m\pi}{L_x}x\right) \equiv |xm\rangle, \tag{9}$$

$$f_{0y,n}(y) = \sqrt{\frac{2}{L_y}}\sin\left(\frac{n\pi}{L_y}y\right) \equiv |yn\rangle, \tag{10}$$

with n, m integers, and

$$\lambda_{0,mn}^2 = -\frac{\hbar^2}{2}\left[\left(\frac{m\pi}{L_x}\right)^2 + \left(\frac{n\pi}{L_y}\right)^2\right]. \tag{11}$$

Hence, for the first term in $H_{xy,1}$, second-order perturbation theory must be used. The second term in $H_{xy,1}$ does, however, contribute in first-order perturbation theory.

The eigenvalue changes due to $H_{xy,1}$ now become

$$\Delta\lambda_{mn}^2 = \lambda_{mn}^2 - \lambda_{0,mn}^2 = -\tfrac{1}{2}e^2B^2\langle xm|x^2|xm\rangle + \hbar^2e^2B^2\sum_{(m',n')\neq(m,n)}\frac{|\langle xm|x|xm'\rangle|^2|\langle yn|\frac{\partial}{\partial y}|yn'\rangle|^2}{\lambda_{0,mn}^2 - \lambda_{0,m'n'}^2}. \tag{12}$$

Having obtained the separation constants λ_{mn}, we can solve for the z-dependent part $g(z)$ in equation (3):

$$\left(-\frac{\hbar^2}{2}\frac{\partial}{\partial z}\frac{1}{m_e(z)}\frac{\partial}{\partial z} + V_{\rm conf}(z) \pm \frac{1}{2}g^*(z)\mu_B B - E - \frac{\lambda_{mn}^2}{m_e(z)}\right)g(z) = 0. \tag{13}$$

The effective potential barrier $V_{\rm barr}$ can be immediately read off from the latter equation as

$$V_{\rm barr} = V_{\rm conf,1} \pm \frac{1}{2}g_1^*\mu_B B - \frac{\lambda_{mn}^2}{m_{e,1}} - \left(V_{\rm conf,2} \pm \frac{1}{2}g_2^*\mu_B B - \frac{\lambda_{mn}^2}{m_{e,2}}\right), \tag{14}$$

where suffices 1 and 2 on m_e, g^*, $V_{\rm conf}$ denote their values in the material constituents 1 and 2 forming the quantum-wire superlattice along the z direction, respectively. This expression is interesting as it shows that the localization of the envelope function along the z direction, determined essentially by the effective potential barrier, depends on the lateral dimensions L_x and L_y of the quantum-wire superlattice (through the λ_{mn}^2 term) and the magnetic-field strength B in addition to the well-known barrier potential due to conduction band edge material discontinuity. We shall soon address this effect in more detail.

The matrix elements appearing in equation (12) can be readily calculated, obtaining for the λ_{mn}^2 change of the ground state with suffices $n = 1, m = 1$:

$$\Delta\lambda_{11}^2 = \left(\frac{1}{4\pi^2} - \frac{1}{6}\right)e^2B^2L_x^2 + \frac{8}{3}\frac{64^2}{9^2\pi^6}e^2B^2\frac{L_x^4}{L_x^2 + L_y^2}, \tag{15}$$

keeping only the lowest contributing state $(m', n') = (2, 2)$ in the second-order perturbation-term summation, which is reasonable since we have assumed that unperturbed states are well separated. Note that if all terms were included in the second-order perturbation expansion of equation (12), symmetry in the dependence of $\Delta\lambda_{mn}^2$ on the L_x and L_y lateral dimensional values results since the magnetic field is applied along the z axis. This symmetry is, due to our approximation in keeping only the first term in the second-order perturbation expansion, almost found for $\Delta\lambda_{11}^2$ in equation (15) since the first-order perturbation-term coefficient $\frac{1}{4\pi^2} - \frac{1}{6}$ is -0.1413 while the second-order perturbation-term coefficient $\frac{8}{3}\frac{64^2}{9^2\pi^6}$ is $+0.1402$.

The ground-state barrier potential can now be written as (combining equations (11), (12), (14) and (15))

$$V_{\mathrm{barr}} = V_{\mathrm{conf},1} - V_{\mathrm{conf},2} + \frac{\hbar^2}{2}\left[\left(\frac{\pi}{L_x}\right)^2 + \left(\frac{\pi}{L_y}\right)^2\right] \times \left(\frac{1}{m_{\mathrm{e},1}} - \frac{1}{m_{\mathrm{e},2}}\right) - \Delta\lambda_{11}^2\left(\frac{1}{m_{\mathrm{e},1}} - \frac{1}{m_{\mathrm{e},2}}\right) \pm \tfrac{1}{2}\left(g_1^* - g_2^*\right)\mu_{\mathrm{B}}B. \qquad (16)$$

3. Strain considerations

Many semiconductor heterostructures are strained and hence contributions to the electron one-band equation from strain must be accounted for. The strain contribution for electrons in cubic crystals is

$$H_{\mathrm{strain}} = D_{\mathrm{e}}\left(\epsilon_{xx} + \epsilon_{yy} + \epsilon_{zz}\right), \qquad (17)$$

where D_{e} is the electron deformation potential and ϵ_{ii} are the strain-tensor diagonal components. For pseudomorphic growth along the z direction of a film on a substrate, the strain is zero in the substrate but nonzero in the film layer. In fact, the lattice-constant (a) mismatch between the film and the substrate defined by

$$\frac{a^{\mathrm{film}} - a^{\mathrm{substrate}}}{a^{\mathrm{substrate}}}, \qquad (18)$$

leads to strain-tensor diagonal components in the film layer equal to

$$\epsilon_{xx} = \epsilon_{yy} = -\frac{a^{\mathrm{film}} - a^{\mathrm{substrate}}}{a^{\mathrm{substrate}}} = \epsilon_{\parallel}, \qquad (19)$$

$$\epsilon_{zz} = \frac{-2c_{12}}{c_{11}}\epsilon_{\parallel}, \qquad (20)$$

where c_{12} and c_{11} are elastic-stiffness tensor components. Thus, the strain contribution to the conduction band effective Hamiltonian becomes

$$H_{\mathrm{strain}} = 2D_{\mathrm{e}}\left(1 - \frac{c_{12}}{c_{11}}\right)\epsilon_{\parallel}. \qquad (21)$$

For typical semiconductors, the deformation potential is approximately 10 eV and the lattice mismatch can be several percent. Hence, the strain effect when it is present usually is of immense importance for the effective barrier potential. Adding H_{strain} to the Hamiltonian in equation (1) and repeating the steps that led to equation (14) now yields

$$V_{\mathrm{barr,strain}} = V_{\mathrm{conf},1} \pm \frac{1}{2}g_1^*\mu_{\mathrm{B}}B - \frac{\lambda_{mn}^2}{m_{\mathrm{e},1}} - \left(V_{\mathrm{conf},2} \pm \frac{1}{2}g_2^*\mu_{\mathrm{B}}B - \frac{\lambda_{mn}^2}{m_{\mathrm{e},2}}\right) + 2D_{\mathrm{e},1}\left(1 - \frac{c_{12,1}}{c_{11,1}}\right)\epsilon_{\parallel,1} - 2D_{\mathrm{e},2}\left(1 - \frac{c_{12,2}}{c_{11,2}}\right)\epsilon_{\parallel,2}, \qquad (22)$$

where again comma-separated suffices 1 and 2 denote the parameter values in the (two) material constituents 1 and 2 forming the quantum-wire superlattice, respectively.

For comparison, we also give the expressions for the electron effective barrier potential $V_{\mathrm{barr,strain}}$ in the cases without strain contributions ($V_{\mathrm{barr}}^{\mathrm{LTB}}$), without strain and magnetic-field contributions ($V_{\mathrm{barr}}^{\mathrm{LT}}$), and the conduction band edge discontinuity ($V_{\mathrm{barr}}^{\mathrm{L}}$). These barrier potentials are given by

$$V_{\mathrm{barr}}^{\mathrm{LTB}} = V_{\mathrm{conf},1} \pm \frac{1}{2}g_1^*\mu_{\mathrm{B}}B - \frac{\lambda_{mn}^2}{m_{\mathrm{e},1}} - \left(V_{\mathrm{conf},2} \pm \frac{1}{2}g_2^*\mu_{\mathrm{B}}B - \frac{\lambda_{mn}^2}{m_{\mathrm{e},2}}\right), \qquad (23)$$

$$V_{\mathrm{barr}}^{\mathrm{LT}} = V_{\mathrm{conf},1} - \frac{\lambda_{mn,0}^2}{m_{\mathrm{e},1}} - \left(V_{\mathrm{conf},2} - \frac{\lambda_{mn,0}^2}{m_{\mathrm{e},2}}\right), \qquad (24)$$

$$V_{\mathrm{barr}}^{\mathrm{L}} = V_{\mathrm{conf},1} - V_{\mathrm{conf},2}, \qquad (25)$$

where, in the superscripts, L corresponds to longitudinal, T to transverse and B to magnetic confinement.

4. Results and discussions

In this section, we compute the electron effective barrier potential for some typical zinc-blende semiconductor quantum-wire heterostructures. In table 1, material parameters used in the calculations are given.

In figure 1, the electron effective potential $V_{\mathrm{barr,strain}}$ is shown as a function of the magnetic-field strength B for a quantum-wire superlattice structure with AlAs as the substrate and GaAs as the film layer. The lateral quantum-wire dimensions are assumed to be $L_x = L_y = 20$ nm, which is typical of what is grown. The in-plane strain in the GaAs film layer is equal to 0.14% and hence strain contributes a small amount of approximately 10.6 meV to the effective barrier potential. Notice that the magnetic-field contribution to $V_{\mathrm{barr,strain}}$ corresponds to approximately -15 meV (-17.5 meV) at $B = 20$ T for spin-up and spin-down polarized electrons, respectively. The strain contribution can be seen to be only approximately 10 meV (the difference between the dashed and circular curves at $B = 0$) for this heterostructure. Note also that the strain contribution does not depend on the lateral quantum-wire dimensions and hence is of equal importance in quantum-well superlattices! For the parameters chosen and up to a magnetic field of 20 T, we see that there is no inversion in the spatial localization.

Table 1. Material parameters taken from [12] except for electron g-factor values which are from [13]. We note that the g-factor value of AlAs is found using a linear extrapolation to $x = 1$ based on data in figure 4 of [14]. The conduction band edge is $V_{\mathrm{conf}} = E_{\mathrm{g}} - \mathrm{VBO}$. Thus, the conduction band edge discontinuity ΔE_{c} between materials 1 and 2 is $V_{\mathrm{conf},1} - V_{\mathrm{conf},2}$.

	E_{g} (eV)	VBO (eV)	$\frac{m_{\mathrm{e}}}{m_0}$	g^*	c_{11} (GPa)	c_{12} (GPa)	a (Å)	D_{e} (eV)
GaAs	1.519	−0.80	0.067	−0.445	1221	566	5.6523	−7.17
AlAs	3.009	−1.33	0.15	2.168	1250	534	5.6611	−5.64
InAs	0.417	−0.59	0.026	−17.5	833	453	6.0583	−5.08
InP	1.4236	−0.94	0.0795	1.48	1011	561	5.8697	−6.0
GaSb	0.812	−0.03	0.039	−9.1	884	403	6.0959	−7.5
InSb	0.235	0	0.0135	−51.3	685	374	6.4794	−6.94

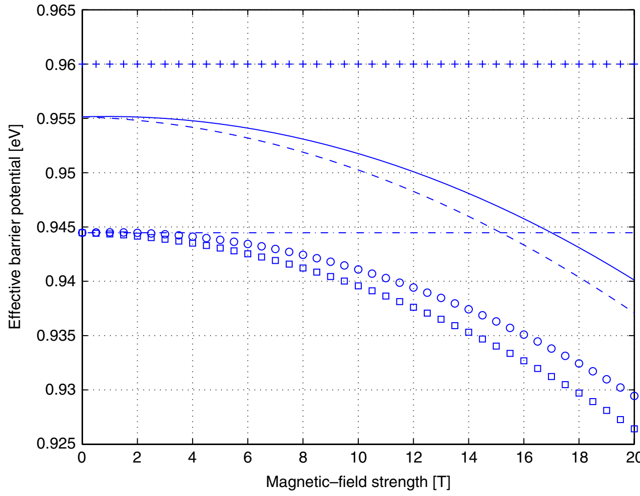

Figure 1. The electron effective potential $V_{\mathrm{barr,strain}}$ for a quantum-wire superlattice structure with AlAs as the substrate and GaAs as the film layer. The six curves correspond to:
(1) $V_{\mathrm{barr,strain}}$—spin-up electron polarization (solid),
(2) $V_{\mathrm{barr,strain}}$—spin-down electron polarization (dashed),
(3) $V_{\mathrm{barr}}^{\mathrm{LTB}}$—spin-up electron polarization (circle),
(4) $V_{\mathrm{barr}}^{\mathrm{LTB}}$—spin-down electron polarization (square), (5) $V_{\mathrm{barr}}^{\mathrm{LT}}$ (dashed–dotted) and (6) $V_{\mathrm{barr}}^{\mathrm{L}}$ (plus). Lateral quantum-wire dimensions are assumed to be $L_x = L_y = 20$ nm.

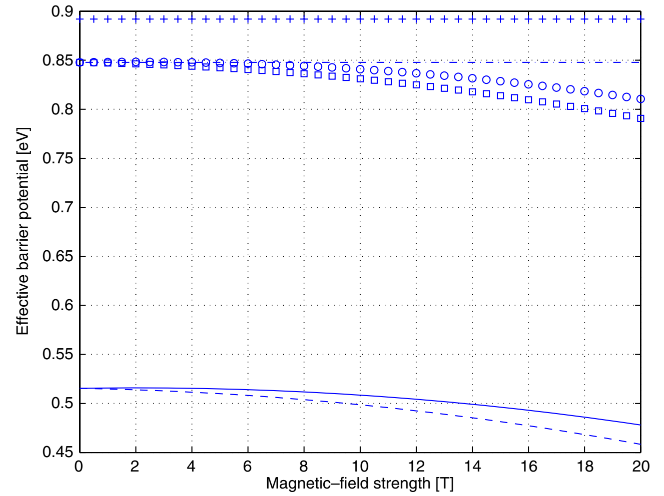

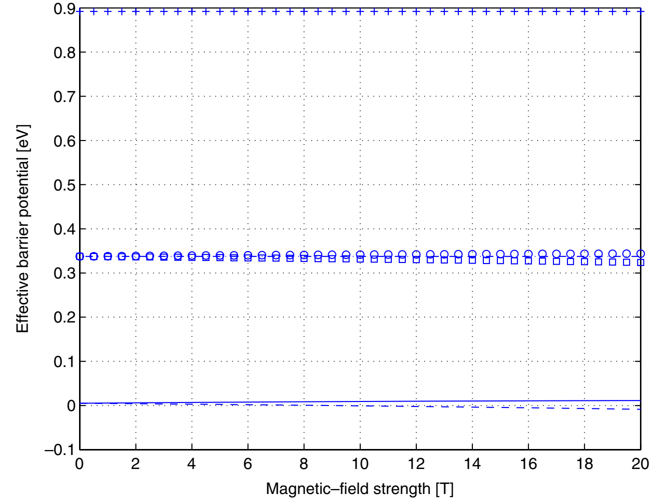

Figure 2. The electron effective potential $V_{\mathrm{barr,strain}}$ for a quantum-wire superlattice structure with GaAs as the substrate and InAs as the film layer. Upper plot is for $L_x = L_y = 20$ nm and lower plot is for $L_x = L_y = 5.65$ nm. Line codings are the same as in figure 1.

Nevertheless, each of the above changes to the effective barrier is comparable to, for example, the excitonic energy and is, therefore, not negligible.

In figure 2 (upper plot), $V_{\mathrm{barr,strain}}$ is shown as a function of B for a quantum-wire superlattice structure with GaAs as the substrate and InAs as the film layer (similar geometrical parameters as in the case above). Notice that the effective electron potential decreases by 40 meV (60 meV) for spin-up (spin-down) polarized electrons to a value of approximately 480 meV (460 meV) as the magnetic field increases from 0 to 20 T. The strain contribution is now very important and amounts to −335 meV for this material combination. While inversion is still not achieved, the corrections to the barrier are now much larger than in the previous example. Indeed, it is important to emphasize that forGaAs/InAs structures, for example, it is possible to reduce the effective barrier potential to nearly zero by stronger lateral confinement. By choosing appropriately the lateral dimensions (for GaAs/InAs quantum-wire superlattices the L_x and L_y can be chosen equal to $L_x = L_y = 5.65$ nm), we can thus control the confinement of spin-up and spin-down polarized electrons in either of the two material layers (InAs or GaAs) in the quantum-wire superlattice (refer to figure 2 (lower plot)). The present work shows clearly that confinement of electrons in quantum-confined structures depends strongly on the actual geometry (size) of the structure besides, obviously, the material constituents. We anticipate that a similar reversal of confinement is likely to take place

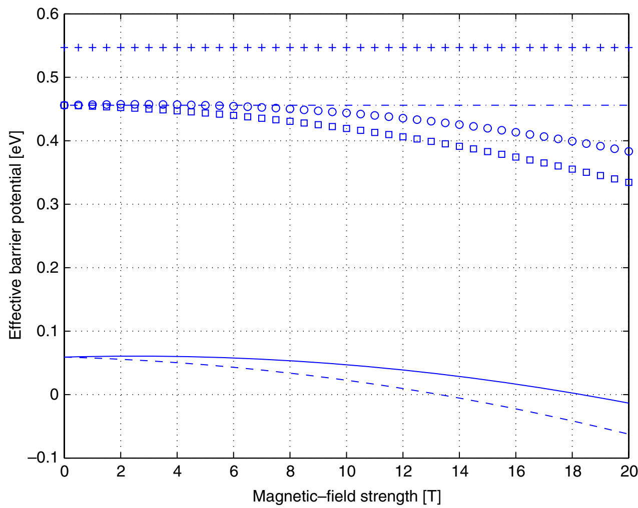

Figure 3. The electron effective potential $V_{\mathrm{barr,strain}}$ for a quantum-wire superlattice structure with GaSb as the substrate and InSb as the film layer. Geometrical parameters and line codings are the same as in figure 1.

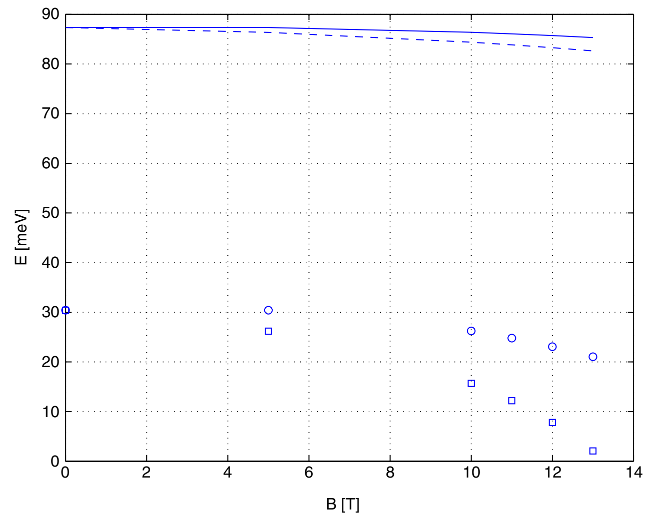

Figure 4. Ground-state energy for a quantum-wire structure with GaSb as the substrate and 10 nm InSb as the film layer. The effective potential of spin-down polarized electrons (including the influence of strain) becomes zero at a magnetic field of approximately 13 T. Hence, we plot energy values up to 13 T. Geometrical parameters and line codings are the same as in figure 1.

also in, for example, InAs/GaAs quantum-dot structures by changing the geometrical parameters (such as the radius of a spherical quantum dot or the radius/length of a cylindrical quantum dot).

In figure 3, for an InSb film grown on a GaSb substrate, it is shown that increasing the magnetic field to approximately 18.2 T (13.5 T) for spin-up (spin-down) polarized electrons leads to a vanishing effective barrier potential. Moreover, $V_{\mathrm{barr,strain}}$ decreases from nearly 59 meV to −13 meV (−69 meV) as the magnetic field increases to 20 T for spin-up (spin-down) polarized electrons. The importance of magnetic-field contributions to the effective potential barrier for this quantum-wire semiconductor heterostructure is thus significant. Moreover, strain contributes approximately −397 meV to the effective barrier potential in this case. Thus, a magnetic field, in practice, can be used to control whether the effective potential is positive or negative in a certain material layer of the quantum-wire heterostructure. For example, tuning the magnetic field around the critical value, 13.5 T, leads to confinement of spin-down electrons either in the InAs layer (below 13.5 T) or the GaAs layers (above 13.5 T). The precise value of the magnetic field is, in a potential device application, determined by the lateral dimensions since the lateral dimensions play an important role for the effective barrier potential (refer to the previous paragraph). Further, since the critical magnetic field for spin-down polarized electrons in the present case is lower than that for spin-up polarized electrons, it is in principle possible by magnetic-field control to separate spin-up and spin-down polarized electrons.

Finally, for the latter material system, we give a calculation of the ground-state energy as a function of the strain and magnetic field, with the same lateral dimensions as before (figure 4). For concreteness, the problem is solved for a single quantum-well structure with an InSb layer thickness of 10 nm. Also, since the InSb/GaSb system has a given strain configuration, the calculation is only done for that value and compared to a fictitious system with zero strain in order to emphasize the role the strain plays. First, in agreement with figure 3, an inversion of the spin-down state is achieved near a magnetic field of 13 T; at that point, a spin splitting of about 20 meV is achieved. Second, the spin splitting for the unstrained system is considerably less, reflecting the nonlinear character of the solutions. In this case, both the phenomena of confinement inversion and spin splitting are aided by the presence of strain and magnetic field. For the influence of inverting the effective potential barrier on nanowire superlattice wavefunctions and localization discussions, we refer the reader to our previous work [11].

5. Conclusions

An effective electron barrier potential analysis is carried out for quantum-wire superlattice structures in the presence of a magnetic field oriented along the quantum-wire superlattice direction and lattice mismatch. It is shown, in the case of InSb/GaSb quantum-wire structures, that magnetic-field values equal to 10 T lead to changes in the effective barrier potential of approximately 25 meV. This value increases almost proportionally with the square of the lateral quantum-wire dimensions and hence becomes important in laterally weakly confined quantum-wire superlattices (or quantum-well superlattices). Strain contributions to the effective electron barrier potential are independent of the lateral dimensions and hence equally important in quantum-well superlattice structures. For InAs/GaAs and InSb/GaSb heterostructures, the strain contribution is strong, amounting to 330 meV and 400 meV, respectively, and hence may force electrons to be confined in the GaAs (GaSb) regions instead of the InAs

(InSb) regions where the conduction band edge potentials are lower. A general conclusion of the present work is that, in the case of a quantum-wire superlattice, the effective electron barrier potential may have dominant contributions from lateral confinement, strain and/or magnetic field. In fact, we have shown that the combination of strain and magnetic-field effects for the InSb/GaSb system can result in confinement inversion for modulated nanowires with realistic lateral dimensions. Moreover, the effective barrier potential can be made spin-dependent by imposing an external magnetic field on the system. As a case example, we demonstrate that, for InAs/GaAs nanowire superlattices, it is possible to tune the effective barrier potential to 0 for cross-sectional dimensions of 5–6 nm by the use of a magnetic field. Finally, since the effective barrier potential is different for spin-up and spin-down polarized electrons, magnetic-field tuning can be used to separate spin-up and spin-down electrons in quantum-wire superlattices. This opens up potential applications in spintronics.

Acknowledgment

MW would like to thank the Department of Physics at Wright State University for their hospitality.

References

[1] Bastard G 1988 *Wave Mechanics Applied to Semiconductor Heterostructures* (Les Ulis: Les Editions de Physique)
[2] Gudiksen M S, Lauhon L J, Wang J, Smith D C and Lieber C M 2002 *Nature* **415** 617
[3] Wu Y, Fan R and Yang P 2002 *Nano Lett.* **2** 83
[4] Björk M T, Ohlsson B J, Sass T, Persson A I, Thelander C, Magnusson M H, Deppert K, Wallenberg L R and Samuelson L 2002 *Nano Lett.* **2** 87
[5] Solanki R, Huo J, Freeouf J L and Miner B 2002 *Appl. Phys. Lett.* **81** 3864
[6] Lew Yan Voon L C and Willatzen M 2003 *J. Appl. Phys.* **93** 9997
[7] Lew Yan Voon L C, Lassen B, Melnik R V N and Willatzen M 2004 *J. Appl. Phys.* **96** 4660
[8] Persson M P and Xu H Q 2006 *Phys. Rev.* B **73** 035328
[9] Gershoni D, Temkin H, Vandenberg J M, Chu S N G, Hamm R A and Panish M B 1988 *Phys. Rev. Lett.* **60** 448
[10] Liu X, Petrou A, Warnock J, Jonker B T, Prinz G A and Krebs J J 1989 *Phys. Rev. Lett.* **63** 2280
[11] Galeriu C, Lew Yan Voon L C, Melnik R V N and Willatzen M 2004 *Comput. Phys. Commun.* **157/2** 147
[12] Vurgaftman I, Meyer J R and Ram-Mohan L R 2001 *J. Appl. Phys.* **89** 5815
[13] Landolt-Börnstein 1982 *Numerical Data and Functional Relationships in Science and Technology* vol 17 (Berlin: Springer)
[14] Hermann C and Weisbuch C 1977 *Phys. Rev.* B **15** 823